

# The effect of sulfur compound on the hydrogenation of tetralin over a Pd–Pt/HDAY catalyst

Huiru Liu<sup>a</sup>, Xiangchun Meng<sup>a</sup>, Dishun Zhao<sup>b</sup>, Yongdan Li<sup>a,\*</sup>

<sup>a</sup> Tianjin Key Laboratory of Applied Catalysis Science and Technology, School of Chemical Engineering, Tianjin University, Tianjin 300072, China

<sup>b</sup> School of Chemical and Pharmaceutical Engineering, Hebei University of Science and Technology, Shijiazhuang 050018, China

Received 24 June 2007; received in revised form 9 November 2007; accepted 9 November 2007

## Abstract

A composite metal catalyst with a Pd/Pt of 4:1 and an H-form dealuminated Y zeolite support for the hydrogenation of tetralin was investigated. The materials were characterized by XRD, NH<sub>3</sub>-TPD, N<sub>2</sub> adsorption, TPR and FTIR. The activity for the hydrogenation of tetralin was investigated with a high-pressure fixed-bed continuous-flow reactor operating at 4.0 MPa. The thiotolerance was tested with feeds containing 200 ppm sulfur in the form of 4,6-dimethylbenzothiophene and thiophene, respectively. It was found that thiophene was more effective for deactivating the catalyst than the former one. The diffusion barrier of the pores for the sulfur compound is likely the major reason for the different deactivation rate of catalysts. The products other than decalins were mainly decalin isomers and ring-opened products. Selectivity of cracking products for the feed with thiophene was lower than that for the other feed, while that of ring-opened and ring-contracted products with the two feeds was similar. © 2007 Elsevier B.V. All rights reserved.

**Keywords:** Tetralin hydrogenation; Pd–Pt catalyst; Zeolite Y; Thiotolerance; Diesel cetane number enhancement

## 1. Introduction

Removal of aromatic compounds in diesel has received considerable attention in recent years because such compounds lower the cetane number and have been recognized as the precursors of particulates in the exhaust gas of the engine [1–4]. Strict regulations limiting the aromatic content have been introduced in several countries [2,3]. A highly active catalyst for aromatic saturation and ring opening is needed. Conventional hydrotreating catalysts if used for this process need severe operating conditions, such as high hydrogen pressure and reaction temperature, which are unfavorable for commercial purpose [1]. Much interest, therefore, has been focused on noble metal catalyst [2,5,6]. However, those are generally poisoned easily by even a few ppm of sulfur in the feedstocks [7]. It has been found that the intrinsic activity and sulfur tolerance can be enhanced by support the metals on a strongly acidic, high surface area support, e.g. zeolite Beta or Y [5,8–12]. Pd/Pt clusters encaged in

the micropores of acidic zeolite Y have been reported to demonstrate higher activity and more interesting sulfur tolerance than monometallic catalysts [2]. Yasuda and Yoshimura [13] confirmed that the coexistence of Pt and Pd in USY zeolite strongly enhances tetralin hydrogenation and improves sulfur tolerance, which depends on the Pd/Pt ratio and reaches a maximum value at a Pd:Pt molar ratio of 4:1. The high sulfur tolerance of the Pd–Pt system is attributed to structural and electronic effects and the formation of Pd–Pt bimetallic particles rather than to the metal dispersion effect. Other supports such as  $\gamma$ -Al<sub>2</sub>O<sub>3</sub>, MCM-41, amorphous SiO<sub>2</sub>–Al<sub>2</sub>O<sub>3</sub> and carbon nanofibers [14–22] have also been explored. Recently, much work on the pore design and the enhancement of the acidity of mesoporous material has been done and a bimodal pore system is assumed superior for the support of this catalyst [23,24]. Meng et al. [23] simulated the molecular dimensions of the aromatic molecules in diesel and found that their minimum cross-sectional diameters are much larger than the crystallographic pore-mouth opening of the supercage of zeolite Y, viz. 0.74 nm. They proposed that the existence of pores with diameters larger than 1.5 nm is necessary to compose a good catalyst for the purpose. This can be obtained by steam and chemical dealumination of zeolite support [25,26].

\* Corresponding author. Tel.: +86 22 27405613; fax: +86 22 27405243.  
E-mail address: ydli@tju.edu.cn (Y. Li).

It has been demonstrated that the sulfur compounds existing in diesel at a sulfur level lower than 500 ppm are mainly substituted thiophenes [27,28]. Those have quite different dynamic diameters. The knowledge on the effect of the molecular dimension and the structure of the sulfur containing compounds is helpful to the design of the catalyst. Since monoaromatics are predominant among the possible aromatic compounds in the hydrotreated light cycle oil, tetralin has been used as a model molecule which is able to diffuse into the supercages of zeolite Y [13,29].

In this work, an H-form dealuminated Y (HDAY) without mesopores is used as the support. Hydrogenation of tetralin is employed as a model reaction over a Pd–Pt/HDAY catalyst in the presence of thiophene (T) or 4,6-dimethyldibenzothiophene (4,6-DMDBT). The effect of the sulfur compound, with different dynamic diameters, on the catalytic activity and product distribution is discussed.

## 2. Experimental

### 2.1. Materials preparation

#### 2.1.1. Dealuminated Y

Commercial NaY powder with Si/Al equal 3 supplied by Shanghai Hengye Molecular Sieve Company Limited was treated with  $\text{SiCl}_4$  at 250 °C for 2 h, with a similar condition to that described by Beyer et al. [30] in order to increase the Si/Al ratio. The  $\text{SiCl}_4$ -treated sample was put into a mixed solution of 2.5 M ammonium acetate and 0.25 M ammonium chloride for ion-exchange. After stirred at 70 °C for 6 h, the material was washed thoroughly. After dried, it was ion-exchanged in 1.0 M ammonium chloride at 70 °C for 3 h and calcined at 550 °C for 5 h. The procedure was repeated for another time. This procedure turned the sample to the acidic form.

#### 2.1.2. Catalyst

The Pd–Pt/HDAY catalyst was prepared by an ion-exchange method.  $\text{Pd}(\text{NH}_3)_4\text{Cl}_2$  and  $\text{Pt}(\text{NH}_3)_4\text{Cl}_2$  were dissolved in 0.02 M  $\text{NH}_3\cdot\text{H}_2\text{O}$ , to form a solution of 0.01 M metal with Pd/Pt = 4. The total amount of metal makes 2.5 wt% in the final catalyst. The solution was added dropwise into a slurry of HDAY with HDAY/water as 1:25 g/ml. The slurry was stirred at 30 °C for another 24 h, with pH 7.0–7.2. After washing and filtering, the catalyst was dried at 80 °C for 10 h. Then the powder was calcined in oxygen flow at 450 °C for 2 h with a ramping 0.8 °C/min.

### 2.2. Characterization

X-ray diffraction (XRD) patterns were taken on a PANalytical X'pert Pro diffractometer using  $\text{Co K}\alpha$  at 40 kV and 40 mA. Before scanning, the sample was maintained in a hydrator with saturated solution of  $\text{CaCl}_2\cdot 6\text{H}_2\text{O}$  for 24 h. The unit cell parameter of NaY and HDAY,  $a_0$ , was determined as described in ASTM D-3942-97 [31]. The number of framework aluminum  $N_{\text{Al}}$  was calculated from  $a_0$  using the Breck–Flanigen equation [32]. Temperature programmed desorption (TPD) of ammonia was

performed on a lab-made equipment with a thermal conductivity detector. 80 mg of zeolite powder in a quartz tube reactor with an internal diameter of 5.5 mm was pretreated at 450 °C for 2 h with argon flow. After cooled to 150 °C, the sample was saturated by a pulsed addition of ammonia. Then the sample was purged in Ar flow at 150 °C for 2 h. Subsequently, the sample was heated linearly to 650 °C at a rate of 10 °C/min. The desorbed ammonia was absorbed from the tail gas with 0.0091 M HCl solution, and was titrated. The nitrogen adsorption–desorption isotherms was determined at –196 °C with a Thermo Finnigan Sorptomatic 1990 instrument. The sample was pressed into tablets, crushed and sieved into grains with a size of 20–40 meshes before use. FTIR spectra were recorded on a NICOLET Nexus spectrometer using the KBr wafer technique. Energy Dispersive Spectroscopy (EDS) analysis of the localized composition was performed with a Philips XL-30 SEM instrument. TPR of the catalyst was carried out on a Thermo Finnigan TPDRO 1100 instrument with a  $\text{H}_2/\text{N}_2$  ( $\text{H}_2$  5%) mixture at a flow rate 20 ml/min (STP). 0.10 g sample was placed in a quartz tube, and heated at a rate of 10 °C/min to 800 °C. A Pyris Diamond TG/DTA was employed to measure the weight loss during oxidation in air. 8 mg sample was heated to 800 °C at a rate of 10 °C/min with an air flow of 20 ml/min (STP). Two samples with adsorption of tridecane and tetralin on the reduced catalyst was prepared at 280 °C with introduction of the adsorbent by a saturation of nitrogen flow of 40 ml/min at room temperature for 1 h.

### 2.3. Catalytic activity

The catalytic activity was measured in a fixed-bed continuous-flow reactor. The clean feed contained 30 wt% tetralin and 70 wt% tridecane. For the feeds with sulfur, T or 4,6-DMDBT was added making a sulfur concentration of 200 ppm. Activity tests were performed using 0.20 g of catalyst in 40–60 meshes diluted with 0.40 g SiC. On top and at the bottom of the catalyst bed extra SiC was filled. The reaction was done at 4.0 MPa, 280 °C, liquid feed flow rate 4.0 ml/h, weight hourly space velocity (WHSV)  $16\text{ h}^{-1}$  and a  $\text{H}_2$ /tetralin ratio of 14.7 (mol). A blank experiment with tridecane was performed with the same conditions. The conversion was 31.3%. The major products were mostly the isomerization products, such as methyl-dodecanes, dimethyl-hendecanes, ethyl-hendecanes, in addition, there exist very small amount of undecanes, such as dodecane and hendecane. Among the products, the isomerization products were over 75 wt%. However, when tridecane was cofeeded with tetralin, the conversion of tridecane was found below 1%. In the calculation of yields for tetralin hydrogenation, the products of tridecane were eliminated by the GC program. To compare the selectivity at a similar tetralin conversion one experiment was performed with clean feed and a liquid weight hourly space velocity  $80\text{ h}^{-1}$ . Prior to catalytic testing, the precalcined sample was treated in a hydrogen stream with 60 ml/min at 101.3 kPa at 350 °C for 2 h. The liquid products of the reaction were collected each 30 min with a 0 °C ice-water trap, and analyzed using an Agilent 6890N GC equipped with a FID and a HP-PONA methyl siloxane capillary column.

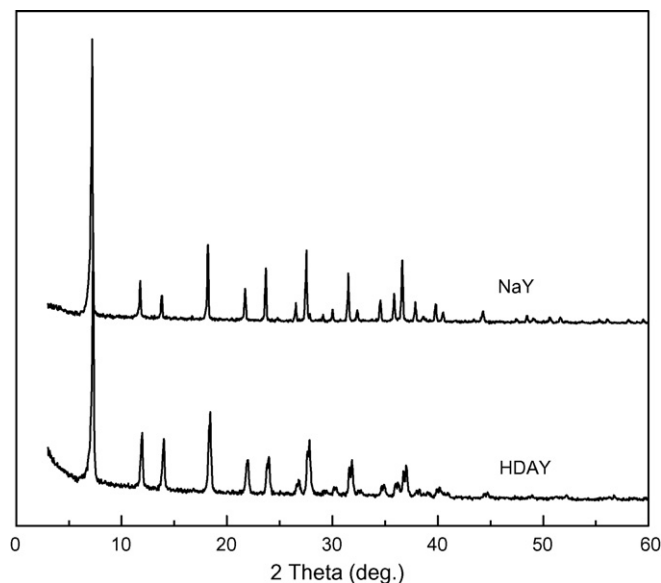


Fig. 1. The XRD patterns of NaY and HDAY.

### 3. Results

#### 3.1. Material property

The XRD patterns of the HDAY and the original NaY are presented in Fig. 1. It displays that although the peak positions are not modified much, however, the peaks are broadened after the dealumination and ion-exchange procedures, which means the HDAY has a smaller particle size. The  $N_{Al}$  and  $a_0$  determined by XRD are listed in Table 1. As observed, these values are modified after dealumination.

Table 1  
Textural and structural properties of the modified Y zeolite

Sample	$a_0$ (Å)	$N_{Al}$	Acid amount ( $\mu\text{mol g}^{-1}$ ) (total <sup>a</sup> )	Pore volume ( $\text{cm}^3 \text{g}^{-1}$ )	
				Micro.	Meso. + surface
HDAY	24.43	28	$1.08 \times 10^3$	0.31	0.04
NaY	24.67	56	–	0.33	0.04

<sup>a</sup> Obtained from titration.

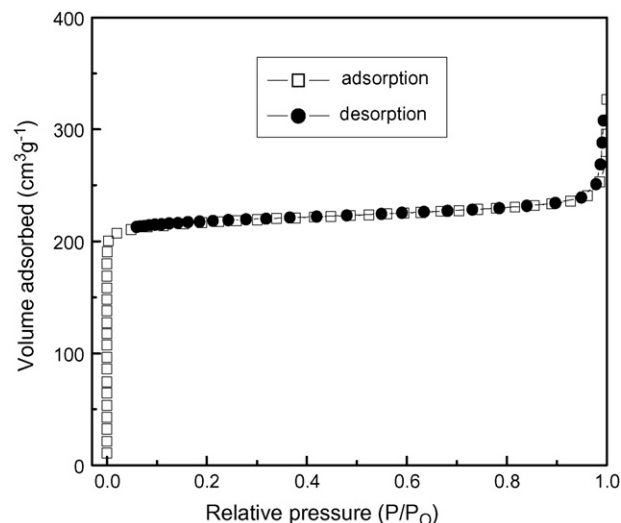


Fig. 3. Nitrogen adsorption–desorption isotherms of HDAY at  $-196^\circ\text{C}$ .

The SEM micrographs of NaY and HDAY are shown in Fig. 2. HDAY presents smaller crystals. The nitrogen adsorption and desorption isotherms at  $-196^\circ\text{C}$  of HDAY are plotted in Fig. 3. A type I isotherm is obtained [33]. Pore volume data of micropores and mesopores given in Table 1 show that these are very similar for the HDAY and that of the parent NaY.

Fig. 4 plots the  $\text{NH}_3$ -TPD curve of the HDAY support, which has only one desorption peak with a starting point at  $160^\circ\text{C}$  and ending at  $630^\circ\text{C}$  and a maximum at around  $350^\circ\text{C}$ . The amount of the acid sites obtained from titration is also given in Table 1.

Fig. 5 compares the FTIR spectra of NaY and HDAY. The spectra of HDAY shows a shift of the peaks of vibrations ( $746 \text{ cm}^{-1}$ ,  $825 \text{ cm}^{-1}$ ,  $1065 \text{ cm}^{-1}$  and  $1190 \text{ cm}^{-1}$ ) in symmetric stretch and asymmetric stretch region [34]. Vibrations of

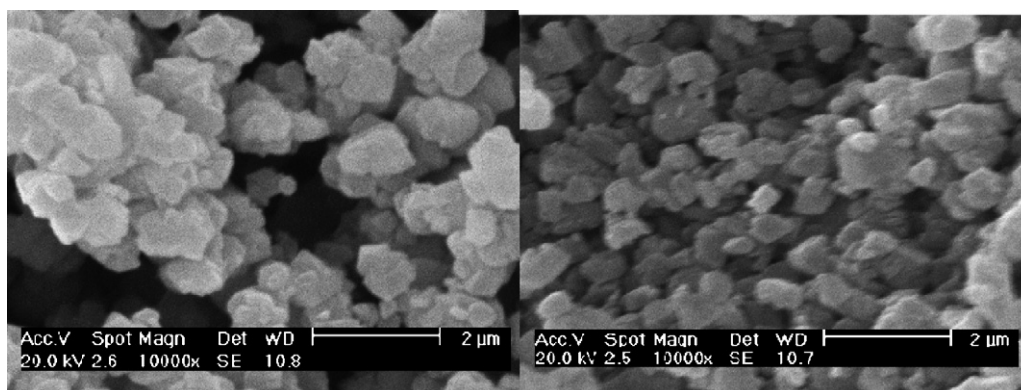
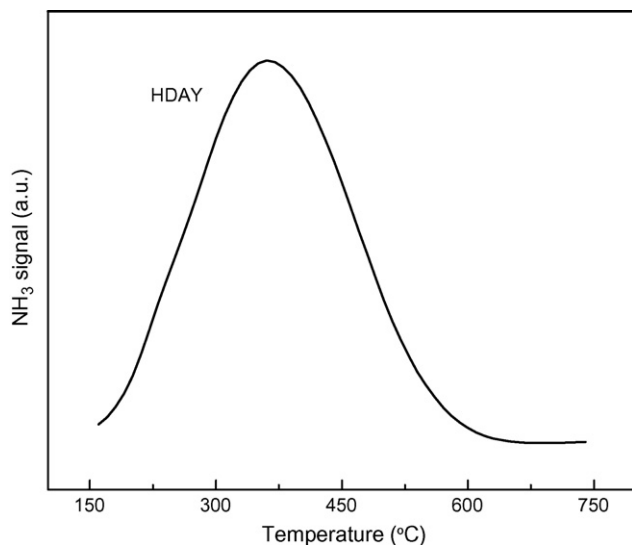


Fig. 2. The SEM micrographs of NaY and HDAY. (Left) NaY, (right) HDAY.

Fig. 4. NH<sub>3</sub>-TPD profiles of HDAY.

double (dbl) rings is also shifted, i.e. the peaks at  $600\text{ cm}^{-1}$  and  $522\text{ cm}^{-1}$  [34]. The peak intensities of external-tetrahedral vibrations and dbl rings vibrations of  $522\text{ cm}^{-1}$  increase compared to NaY.

The TPR profiles of the support and the calcined Pd–Pt/HDAY catalyst are shown in Fig. 6. No H<sub>2</sub>-consumption peaks are found in the TPR profile of the support, while two peaks located at about 141 °C and 225 °C are observed for the catalyst.

The sulfur content on the surface of the catalyst samples after 9 h reaction was measured with an EDS technique, the result shows that, for the catalyst underwent reaction with clean feed sulfur was not detected, while for the catalysts underwent reactions with both the feeds containing T and DMDBT the sulfur contents were the same and the value was 0.27 at. %.

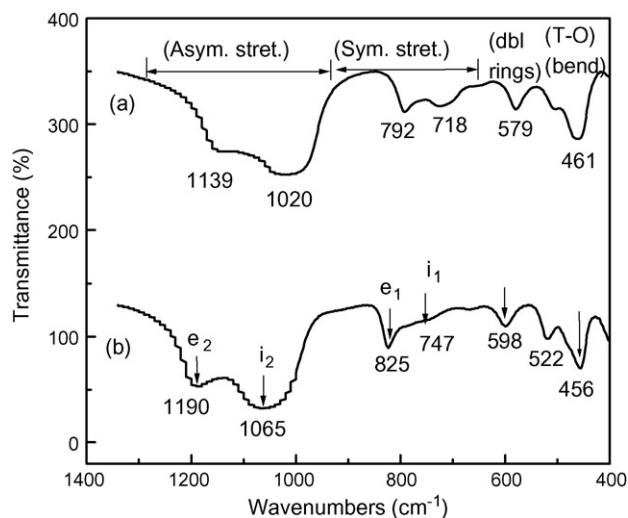


Fig. 5. FTIR spectra of Y zeolites. (a) NaY; (b) HDAY. i: internal (intra-tetrahedral) vibrations; e: external (inter-tetrahedral) vibrations; T: framework cation, e.g. Si or Al; Dbl: double; Asym.: asymmetric; Sym.: symmetric.

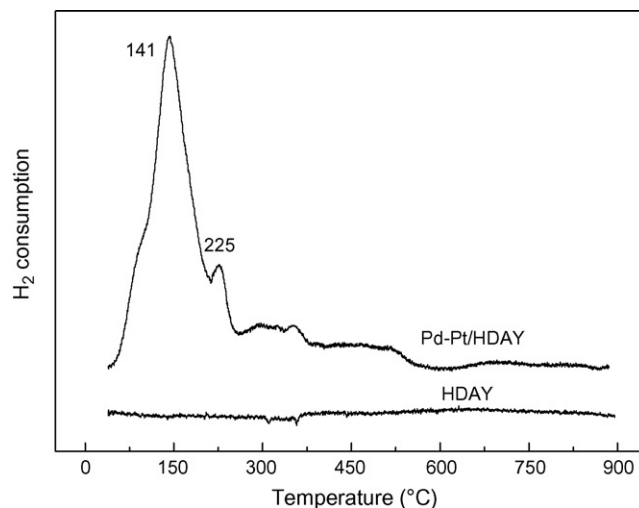


Fig. 6. TPR profiles of Pt–Pd/HDAY catalyst and HDAY support.

Fig. 7 presents the TG and DTA curves of the catalysts after adsorption of tetralin and tridecane. It shows that the adsorption amount of tridecane is much smaller than that of tetralin. Both the adsorbates oxidize at around 200 °C, however, the DTA peak of tridecane is very small, while that of tetralin is very large, indicating that the oxidation of tridecane is very limited. The DTA curve of the catalyst underwent 9 h reaction in clean feed is illustrated in Fig. 8, which is similar as that of the sample adsorbed tetralin shown in Fig. 7. The DTA curves for the samples underwent reaction with the T and DMDBT feeds are omitted because of the similarity. Fig. 8 gives also three TG curves for the three samples underwent reactions for 9 h in the three different feeds. It is inferred that the weight losses before 200 °C is the desorption and in between 200 °C and 250 °C is the oxidation of tetralin and the intermediates. The weight losses after 250 °C are the oxidation of heavier intermediates or carbon precursors and show a sequence that the sample with T > the sample with DMDBT > the sample with clean feed.

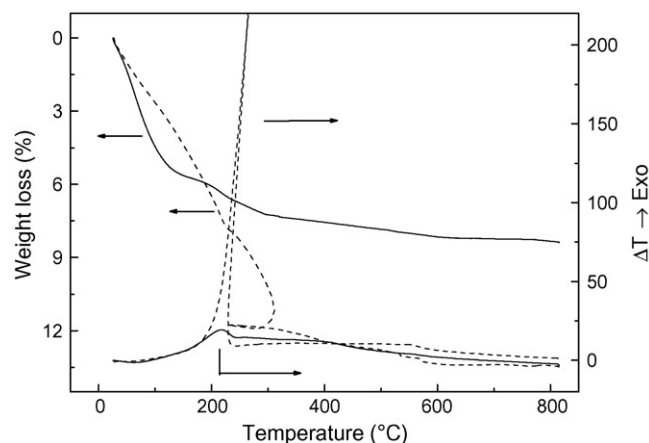


Fig. 7. TG and DTA profiles of catalyst in air after adsorbing reactants. Dashed line: tetralin; solid line: tridecane.

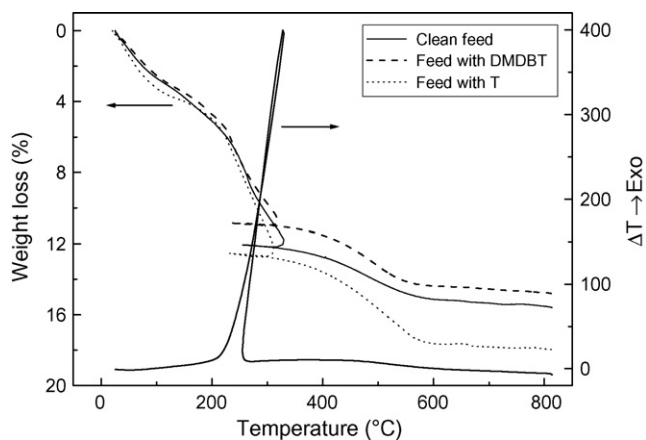


Fig. 8. TG and DTA curves of catalyst samples after 9 h in different feeds. The DTA curve is for the sample obtained with clean feed.

### 3.2. Hydrogenation of tetralin

Tetralin conversion as a function of reaction time in clean feed and sulfur containing feeds are depicted in Fig. 9. For the clean feed, the tetralin conversion is constant and as high as 100%. The conversions with feeds containing sulfur decrease with different rates. Fig. 10 illustrates the curves of the total selectivity of decalins (DECs) with reaction time. For the clean feed, the selectivity of DECs is very low, close to 10%, and very stable with time. For the feeds with sulfur, the selectivity of DECs becomes rather high and grows with time, i.e. along with the deactivation happens. For the T containing feed, the selectivity of DECs is always higher than that of the feed with 4,6-DMDBT.

### 3.3. Product distribution

During the reaction, ring-opening (RO), isomerization and hydrogenolysis take place after the hydrogenation of tetralin.

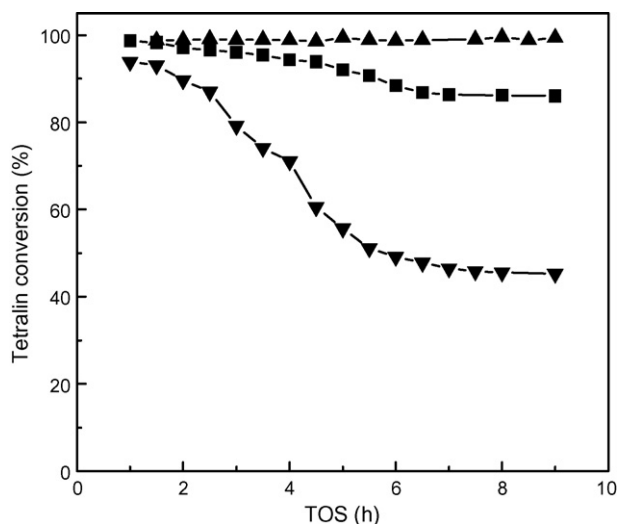


Fig. 9. Conversion of tetralin with time on stream. (▲) Clean feed; (■) 4,6-DMDBT containing feed; (▼) T containing feed.

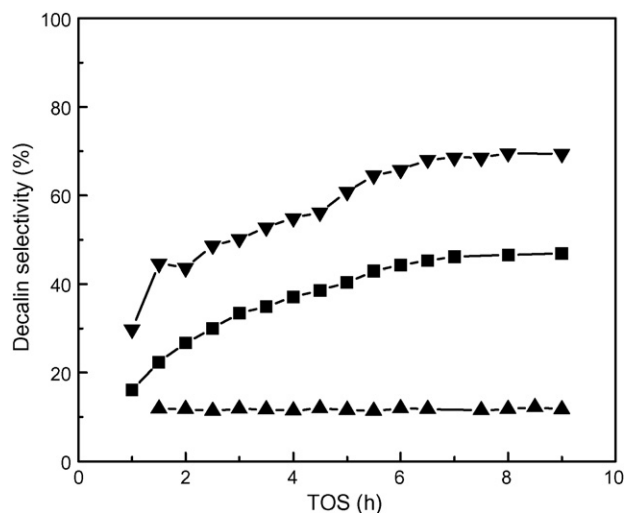


Fig. 10. Selectivity of DECs with time on stream. (▲) Clean feed; (■) 4,6-DMDBT containing feed; (▼) T containing feed.

The products other than DECs are mainly DEC isomers, RO and cracking products.

To facilitate discussion, reaction products are grouped as follows:

- Cracking products: products with fewer carbon atoms than the aromatic feed, i.e.  $\leq C_9$ .
- DEC isomers: usually referred to as ring-contraction product (RC) or DEC isomers. The major ones are: methylbicyclo[4.3.0]nonanes, dimethylbicyclo[4.3.0]nonanes, dimethylbicyclo[3.2.1]octane and methylbicyclo[3.3.1]nonanes.
- Cis*- and *trans*-DECs, generally grouped as DECs.
- RO products, mainly  $C_{10}$ -alkylcyclohexanes and  $C_{10}$ -alkylcyclopentanes as: methyl-cyclohexanes, propyl-cyclohexanes, butyl-cyclohexanes, ethyl-cyclopentanes.

The reaction results show that the formation of naphthalene,  $C_{11}$  and higher products is negligible. Table 2 summarizes the selectivity of the grouped compounds after 9 h reaction. It shows that when sulfur is present, a significant drop in the selectivity of cracking products is observed, while the selectivity of DECs increased. For the RO products, the selectivity is not much influenced by the sulfur compound. It must be noted that in this work, only the liquid composition collected in a cold trap is given, but the light products are neglected. This was supported by several experimental efforts to measure the gaseous product. The results show that the light products in gas phase are negligible. The selectivities of products at a same conversion level, around 86%

Table 2  
Product distribution after reaction for 9 h

Feeds	Selectivity of products (wt%)			
	Cracking products	DECs	RC	RO
Clean feed	51.97	11.73	10.85	23.38
DMDBT feed	19.97	46.90	7.97	24.52
T feed	5.40	69.35	3.62	21.50

Table 3  
Product distribution at a similar conversion level

Feeds	Conversion of tetralin (%)	Selectivity of products (wt%)			
		Cracking products	DECs	RC	RO
Clean feed	85.02	25.34	39.52	10.14	25.00
DMDBT feed	86.07	19.97	46.90	7.97	24.52
T feed	87.02	15.26	48.68	7.23	28.83

are summarized in Table 3. The selectivity of cracking products for the three feeds is quite different, while for the RO and RC products, the selectivities are similar.

## 4. Discussion

### 4.1. Structure of support

DAY without mesopores as a support provides information on the shape selectivity. In this work, the HDAY is obtained by  $\text{SiCl}_4$ -treatment. The nitrogen adsorption and desorption isotherms demonstrate that no mesopores present. The XRD patterns show that the material keeps the structure of the original NaY, with a reduction of the framework aluminum and particle size. The FTIR spectra of HDAY exhibit a shift of the peaks towards the blue end except for the T–O bending vibration, which indicates the increase of  $\text{SiO}_2/\text{Al}_2\text{O}_3$  ratio in the framework. This is in consistency with the result determined by XRD. The  $\text{NH}_3$ -TPD profiles and data in Table 1 show that the amount of acid sites on the HDAY is still large and the acid strength distribution is rather wide.

The location of Pd, Pt ions in faujasite zeolites is determined by the pretreatment conditions [9]. As it has been recognized, the reduction temperature of the metal ions depends on their location in the zeolite, i.e. in the sodalite,  $\beta$  cage and supercage of the crystal. According to the interpretation of Tzou et al. [35], the large reduction peak in TPR profile at 141 °C is attributed to the reduction of  $\text{Pd}^{2+}$ ,  $\text{Pt}^{2+}$  in the supercage.

### 4.2. Tetralin hydrogenation

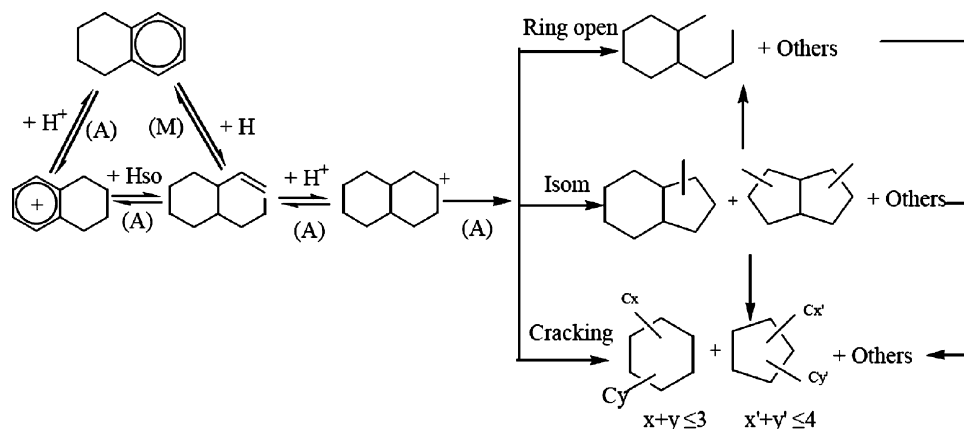
The results presented in Fig. 9 show that sulfur in T feed are more effective for deactivating the catalyst than that in 4,6-DMDBT feed. Fig. 10 shows that the DEC's selectivity with T feed is always higher than that with the feed containing 4,6-DMDBT, indicating that the catalyst is poisoned more deeply by sulfur in T feed than that in latter. However, EDS measurements result in that the sulfur atomic contents on the surface of the samples underwent reactions with different sulfur containing feeds are exactly the same, viz. 0.27%, which indicates that the amount of sulfur adsorbed is not a major factor for deactivation. The weight loss measured by TG of the sample after reaction in T feed is much larger than that of the sample reacted with DMDBT feed. The TG curve obtained with the sample reacted with the clean feed is more closer to that of the curve with the sample reacted with the DMDBT feed. The weight losses of the samples after worked in sulfur containing feeds are obvi-

ously larger than that of worked in clean feed, and that of the sample with T is larger than that with DMDBT. These results indicate that less active catalyst for hydrogenation is easier to form coke precursors. The difference in the deactivation rate may be attributable to the deactivation of the metal sites in supercages which display the size effect of the pores and the molecules. The size of 4,6-DMDBT, 0.87 nm  $\times$  12.2 nm [23], is much larger than the Y supercage openings, viz. 0.74 nm, it is reasonable to assume that the molecule is difficult to access the active sites engaged in the supercages. The size of T molecule is simulated as 0.67 nm  $\times$  0.72 nm, which can enter the cages and thus poison the active sites inside the supercage. The supercage confined metal clusters, evidenced here by TPR, are likely acting as the active sites for hydrogenation of aromatics with smaller dimensions than the cage openings, as well as a source of spilt-over hydrogen to recover the poisoned metal sites located in pores accessible to 4,6-DMDBT and to facilitate the hydrogenation of the molecules adsorbed on the acid sites outside the supercages. It has been proposed that acid sites can be involved in the rate-determining steps of the hydrogenation reactions [36]. However, one may argue that desulfurization happens under the same condition and the  $\text{H}_2\text{S}$  is accessible to the supercage confined metal clusters. There is evidence that  $\text{H}_2\text{S}$  is less poisonous than the thiophenic compounds [37].

### 4.3. Product distribution

The possible reaction pathways are proposed in Scheme 1. Zeolites are not super acids and cannot protonate an alkane. The reaction of decalin to its cation cannot occur, but should go via an olefin first. Therefore, in Scheme 1, tetralin is first hydrogenated on the metal sites to produce an intermediate, or hydrogenated on acid sites with the spilt-over hydrogen, which is similar to that proposed in Ref. [38]. The intermediate is protonated on the Brönsted sites, followed by RC of the saturated  $\text{C}_6$  ring to a  $\text{C}_5$  ring, which can continue to produce the corresponding  $\text{C}_{10}$ -RO product. Moreover, as shown in the Scheme,  $\text{C}_{10}$ -RO products can also be formed from protonated decalin on Brönsted sites. Cracking reactions occur simultaneously from the decalins, RO and RC products. From the Scheme, it is proposed that the deactivation of acid sites affects the product distribution.

It has been shown that the existence of Pd and Pt metals suppress the fast deactivation of zeolite Y [39]. Sulfur poisons the metal sites by forming stable sulfide which displays much lower hydrogen dissociation ability than the corresponding metals. As a consequence, the rate of desorption and hydrogenation



Scheme 1. Reaction path of tetralin on metal catalyst. M: metal sites; A: acid sites; Hso: spilt-over hydrogen.

of intermediates adsorbed on the acid sites is not enough fast to prevent coking or condensation due to the lowered spilt-over hydrogen concentration on the surface. This deactivates the acid sites [40,41]. The effect of T and 4,6-DMDBT feed on the product distribution can be explained within this context. T poisons the metal sites faster than 4,6-DMDBT, and lowers hydrogen activation ability more effectively. This leads to a decreased amount of spilt-over hydrogen. As a consequence, the acid sites recovery is hampered and the rate of coking or condensation increased. This is in consistency with the TG-DTA result, although this technique gives a global weight loss, which includes different adsorbed species. It has been proposed that the average lifetime of adsorbed carbonium ions is longer on stronger acid sites, increasing the probability of condensation [42]. Therefore, coking deactivates first the strongest acid sites and inhibits the cracking products and improves the selectivity of DEC's [43–45]. Therefore, the selectivity to cracking products for the 4,6-DMDBT feed is in between those of the clean and T feeds.

Kubička et al. [46] proposed a mechanism for RO of decalin over acidic catalyst, supposing that the active species are the adsorbed carbonium ions as shown in Scheme 1, which undergo isomerization and  $\beta$ -scission, thus yield skeletal isomers of decalin and RO products. Here, the selectivity of RC is low. It is likely that the RC products, if formed, may crack rapidly into RO products. The data in Table 3 show that the selectivity to cracking product has much larger difference for different feeds than that of RO and RC products. It is likely that the cracking products form mainly on strong acid sites, while the RO and RC reactions can be achieved on strong and middle strength acid sites, as it is informed that sulfur has a weaker effect on RO and RC products than on cracking product.

## 5. Conclusions

A Pd–Pt catalyst supported on HDAY without mesopores was used to assess the difference of the poisoning effect of T and 4,6-DMDBT. Various characterization techniques show that the support material kept the structure of zeolite Y, however, with the decrease of the particle size and the Al/Si ratio. The support

is still very acidic with a large amount of acid sites and a wide range of acid strength distribution. The results of tetralin hydrogenation reaction show that T is more effective for deactivating the catalyst than 4,6-DMDBT, which is attributed to the shape selectivity of the molecular sieve and the different poisoning ability for hydrogen dissociation sites of the two compounds. Due to the different poisoning effect of T and 4,6-DMDBT on the metal sites, and in consequence the different recovery rate of acid sites due to the different amount of spilt-over hydrogen for the two feeds, the results show that the sulfur compound influences the product selectivity. The selectivity to cracking product for the 4,6-DMDBT feed are between those of the clean and T feeds. At the same conversion level in different feeds, the selectivity to cracking product has much larger difference for the three feeds than that of RO and RC products.

## Acknowledgements

This work has been supported by the Natural Science Foundation of China under contract number 20425619. The work has been also supported by the Program of Introducing Talents to the University Disciplines under file number B06006, and the Cheung Kong Scholar Program for Innovative Teams of the Ministry of Education under file number IRT0641.

## References

- [1] J.P. van den Berg, J.P. Lucien, G. Germaine, G.L.B. Thielemans, *Fuel Proc. Technol.* 35 (1993) 119.
- [2] A. Stanislaus, B.H. Cooper, *Catal. Rev. Sci. Eng.* 36 (1994) 75.
- [3] B.H. Cooper, B.B.L. Donniss, *Appl. Catal. A* 137 (1996) 203.
- [4] D.P. Liu, Y.D. Li, *Prog. Chem.* 16 (2004) 891 (China).
- [5] C.H. Bartholomew, P.K. Agarwal, J.R. Katzer, *Adv. Catal.* 31 (1982) 135.
- [6] B.H. Cooper, A. Stanislaus, P.N. Hannerup, *Hydrocarb. Process.* 72 (1993) 83.
- [7] J. Barbier, E. Lamy-Pitara, P. Marecot, J.P. Boitiaux, J. Cosyns, F. Verna, *Adv. Catal.* 37 (1990) 279.
- [8] J.A. Rabo, V. Schomaker, P.E. Pickert, *Proceeding of the 3rd Int. Congr. on Catalysis, Amsterdam, North Holland, Paper II.4, 1965, p. 1264.*
- [9] P. Gallezot, *Catal. Rev. Sci. Eng.* 20 (1979) 121.
- [10] N. Matsubayashi, H. Yasuda, M. Immamura, Y. Yoshimura, *Catal. Today* 45 (1998) 375.

- [11] C.C. Costa Augusto, J.L. Zotin, A. da Costa Faro, *Catal. Lett.* 75 (2001) 37.
- [12] B. Pawelec, R. Mariscal, R.M. Navarro, S.V. Bokhorst, S. Rojas, J.L.G. Fierro, *Appl. Catal. A* 225 (2002) 223.
- [13] H. Yasuda, Y. Yoshimura, *Catal. Lett.* 46 (1997) 43.
- [14] J.F. Chiou, Y.L. Huang, T.B. Lin, J.R. Chang, *Ind. Eng. Chem. Res.* 34 (1995) 4277.
- [15] T.B. Lin, C.A. Jan, J.R. Chang, *Ind. Eng. Chem. Res.* 34 (1995) 4284.
- [16] C.A. Jan, T.B. Lin, J.R. Chang, *Ind. Eng. Chem. Res.* 35 (1996) 3893.
- [17] S.D. Lin, C. Song, *Catal. Today* 31 (1996) 93.
- [18] A. Corma, A. Martínez, V. Martínez-Soria, *J. Catal.* 169 (1997) 480.
- [19] M. Vaarkamp, W. Dijkstra, B.H. Reesink, P.H. Berben, *Am. Chem. Soc., Div. Petrol. Chem. Prepr.* 43 (1998) 77.
- [20] T.D. Tang, J.L. Chen, Y.D. Li, *Chin. J. Chem. Phys.* 18 (2005) 1 (China).
- [21] T.D. Tang, J.L. Chen, Y.D. Li, *Acta Phys. Chim. Sin.* 21 (2005) 730 (China).
- [22] T.D. Tang, J.L. Chen, Y.D. Li, *Chem. J. Chin. Univ.* 27 (2006) 129 (China).
- [23] X.C. Meng, Y.X. Wu, Y.D. Li, *J. Porous Mater.* 13 (2006) 365.
- [24] H.J. Zhang, X.C. Meng, Y.D. Li, Y.S. Lin, *Ind. Eng. Chem. Res.* 46 (2007) 4186.
- [25] R.D. Shannon, K.H. Gardner, R.H. Staley, G. Bergeret, P. Gallezot, A. Aroux, *J. Phys. Chem.* 89 (1985) 4778.
- [26] J. Scherzer, *J. Catal.* 54 (1978) 285.
- [27] M.J. Girgis, B.C. Gates, *Ind. Eng. Chem. Res.* 30 (1991) 2021.
- [28] D.D. Whitehurst, H. Farag, T. Nagamatsu, I. Sakanishi, I. Mochida, *Catal. Today* 45 (1998) 299.
- [29] M. Santikunaporn, J.E. Herrera, S. Jongpatiwut, D.E. Resasco, W.E. Alvarez, E.L. Sughrue, *J. Catal.* 228 (2004) 100.
- [30] H.K. Beyer, I.M. Bwlenykaja, F. Hange, M. Tielen, P.J. Grobet, P.A. Jacobs, *J. Chem. Soc., Faraday Trans. I* 81 (1985) 2889.
- [31] American Society for testing and Materials, D3942-97, West Conshohocken, 1997, p. 1.
- [32] D.W. Breck, E.M. Flanigen, *Molecular Sieves*, Society of Chemical Industry, London, 1968, p. 47.
- [33] K.S.W. Sing, D.H. Everett, R.A.W. Haul, L. Moscou, R.A. Pierotti, J. Rouquérol, T. Siemieniowska, *Pure. Appl. Chem.* 57 (1985) 603.
- [34] Q. Xin, C.M. Liang, *Chin. Petrol. Technol.* 30 (2001) 157.
- [35] M.S. Tzou, B.K. Teo, W.M.H. Sachtler, *J. Catal.* 113 (1988) 220.
- [36] P. Chou, M.A. Vannice, *J. Catal.* 107 (1987) 129.
- [37] C.S. Song, *Chem. Technol.* 29 (1999) 26.
- [38] J. Wang, Q.Z. Li, J.D. Yao, *Appl. Catal. A* 184 (1999) 181.
- [39] D. Kubička, N. Kuma, P. Mäki-Arvela, M. Tiitta, V. Niemi, H. Karhu, T. Salmi, D.Y. Murzin, *J. Catal.* 227 (2004) 313.
- [40] J. Barbier, G. Corro, Y. Zhang, J.P. Bournoville, J.P. Franck, *Appl. Catal.* 34 (1987) 147.
- [41] S.K. Sahoo, P.V.C. Rao, D. Rajeshwer, K.R. Krishnamurthy, I.D. Singh, *Appl. Catal. A* 244 (2003) 311.
- [42] A. Corma, P.J. Miguel, A.V. Orchillés, *J. Catal.* 145 (1994) 171.
- [43] M.A. Arribas, A. Martínez, *Appl. Catal. A* 230 (2002) 203.
- [44] M. Sugioka, F. Sado, Y. Matsumoto, N. Maesaki, *Catal. Today* 29 (1996) 255.
- [45] M.A. Arribas, P. Concepción, A. Martínez, *Appl. Catal. A* 267 (2004) 111.
- [46] D. Kubička, N. Kumar, P. Mäki-Arvela, M. Tiitta, V. Niemi, T. Salmi, D.Y. Murzin, *J. Catal.* 222 (2004) 65.